Queuosine Salvage in *Bartonella henselae* Houston 1: A Unique Evolutionary Path

Samia Quaiyum[a%], Yifeng Yuan[a%], Guangxin Sun[b], R. M. Madhushi N. Ratnayake[c*], Geoffrey Hutinet[a@], Peter C. Dedon[b], Michael F. Minnick[d] and Valérie de Crécy-Lagard[a, e*]

[a] Department of Microbiology and Cell Science, University of Florida, Gainesville, FL 32611; [@]Current address: Department of Biology, Haverford College, 370 Lancaster Ave, Haverford, PA

[b] Department of Biological Engineering, Massachusetts Institute of Technology, Cambridge, MA 02139

[c] Department of Chemistry, University of Florida, Gainesville, FL 32611; *Current address: Department of Biochemistry, School of Medicine, Vanderbilt University, Nashville, TN 37232

[d] Division of Biological Sciences, University of Montana, Missoula, Montana, MT 59812

[e] Genetic Institute, University of Florida, FL 32611

[%]Contributed equally

*Corresponding author: vcrecy@ufl.edu

Short title: Queuosine salvage in Bartonella

Abstract

Queuosine (Q) stands out as the sole tRNA modification that can be synthesized via salvage pathways. Comparative genomic analyses identified specific bacteria that showed a discrepancy between the projected Q salvage route and the predicted substrate specificities of the two identified salvage proteins: 1) the distinctive enzyme tRNA guanine-34 transglycosylase (TGT), responsible for inserting precursor bases into target tRNAs; and 2) Queuosine Precursor Transporter (QPTR) , a transporter protein that imports Q precursors. Organisms like the facultative intracellular pathogen *Bartonella henselae*, which possess only TGT and QPTR but lack predicted enzymes for converting $preQ_1$ to Q, would be expected to salvage the queuine (q) base, mirroring the scenario for the obligate intracellular pathogen *Chlamydia trachomatis*. However, sequence analyses indicate that the substrate-specificity residues of their TGTs resemble those of enzymes inserting $preQ_1$ rather than q. Intriguingly, mass spectrometry analyses of tRNA modification profiles in *B. henselae* reveal trace amounts of $preQ_1$, previously not observed in a natural context. Complementation analysis demonstrates that *B. henselae* TGT and QPTR not only utilize $preQ_1$, akin to their *E. coli* counterparts, but can also process q when provided at elevated concentrations. The experimental and phylogenomic analyses suggest that the Q pathway in *B. henselae* could represent an evolutionary transition among intracellular pathogens—from ancestors that synthesized Q *de novo* to a state prioritizing the salvage of q. Another possibility that will require further investigations is that the insertion of $preQ_1$ has fitness advantages when *B. henselae* is growing outside a mammalian host.

Keywords: Queuosine, *Bartonella henselae*, tRNA modification, intracellular parasite, TGT enzyme, YhhQ

Author summary

Transfer RNAs (tRNAs) are adaptors that deliver amino acids to ribosomes during translation of messenger RNAs (mRNAs) into proteins. tRNA molecules contain specially-modified nucleotides that affect many aspects of translation including regulation of translational efficiency, as modified nucleotides primarily occur near the portion of tRNA (anticodon) that directly interacts with the coding sequence (codon) of the

mRNA while it is associated with a ribosome. Queuosine (Q) is a modified tRNA nucleotide located in the anticodon that can be synthesized or uniquely imported from the environment as Q or a precursor using a salvage mechanism. Free-living bacteria, e.g., *E. coli*, can synthesize Q or salvage precursors from the environment, but many obligate intracellular pathogens, e.g., *Chlamydia trachomatis*, cannot synthesize Q and must import a precursor from eukaryotic hosts. In this study, we determined that *Bartonella henselae*, a facultative intracellular bacterial pathogen of vascular cells, falls somewhere in the middle, as it is unable to synthesize Q but can salvage Q or certain precursors. The unusual nature of Bartonella's system suggests different evolutionary scenarios. It could be a snapshot of the transition from Q synthesis to strict Q salvage or represent a unique adaptation to a complex multi-host lifestyle.

Introduction

tRNA modifications fine-tune translation by various mechanisms such as modulating the efficiency or accuracy of translation or affecting tRNA stability (1). Recent studies have revealed that modifications can play key roles in bacterial pathogenesis (2,3). Queuosine (Q) is a modification of the wobble base in tRNAs with GUN anticodons of many bacteria and eukaryotes that can affect both translational efficiency and accuracy depending on the organism (4,5). The *in vivo* significance of this modification has remained enigmatic for decades as it has been lost repeatedly during evolution (6), but recent studies have suggested that it may act as a regulatory component in the translation of proteins derived from genes enriched in TAT codons compared with TAC codons (7,8). In bacteria, Q modification was shown to have roles in oxidative stress, metal homeostasis, and virulence (9–12).

Q is synthesized from guanosine triphosphate (GTP) by bacteria in a complex eight-step pathway fully elucidated in *E. coli* (Fig. 1A). Four enzymes (GCHI, QueD, QueE, and QueC) convert GTP into 7-cyano-7-deazaguanine ($preQ_0$). QueF then reduces $preQ_0$ to 7-aminomethyl-7-deazaguanine ($preQ_1$) that is inserted into tRNAs by tRNA guanine-34 transglycosylase (bTGT) (4). The inserted base $preQ_1$ is converted to Q by two additional steps involving QueA and QueG or QueH, depending on the organism

69 (4,13). It should be noted that Q is the only tRNA modification that can be salvaged or recycled (5).
70 Eukaryotes only use the salvage route and their TGT enzyme, a heterodimeric QTRT1/QTRT2 complex,
71 incorporates the queuine (q) base directly into the target tRNAs (5). The salvage routes in bacteria vary
72 greatly. Some organisms lack the $preQ_0$ or $preQ_1$ pathway genes but encode all the downstream genes and
73 import these precursor bases to finalize Q synthesis *in vivo* (14). This salvage route is also observed in
74 organisms like *E. coli* that can synthesize Q *de novo*. Other bacteria lack all canonical synthesis genes
75 except *tgt* and can salvage q like eukaryotes. Two q salvage routes have been identified in bacteria, to date
76 (15), including the direct salvage route found in the intracellular pathogen *Chlamydia trachomatis*, or the
77 indirect salvage route found in the gut microbe *Clostridioides difficile* (Fig. 1B and C, respectively). In the
78 direct route, the substrate specificity of the *C. trachomatis* bTGT enzyme has shifted to insert q instead of
79 $preQ_1$ like most bacterial homologs (15). In the indirect route, a recently discovered radical enzyme (QueL)
80 can regenerate the $preQ_1$ intermediate from a q precursor that is imported directly or derived from the
81 hydrolysis of the Q nucleoside by QueK (15). Only a few transporters involved in Q salvage pathways have
82 been identified and experimentally characterized. The first was the YhhQ /COG1738 family, now renamed
83 QPTR (Queuosine Precursor Transporter), involved in the transport of $preQ_0$ and $preQ_1$ in *E. coli* and q in
84 *C. trachomatis* (14,15). Members of the Energy-Coupling Factors (ECFs) family had been predicted to be
85 involved in $preQ_0$ and $preQ_1$ transports (15)) and two of the *C. difficile* specificity components (or ECF-
86 QueT) were shown to transport a variety of Q precursors in a reconstituted system (15).

87 The proportion of Q-modified tRNAs can change with the developmental stage in several
88 eukaryotic parasites that undergo complex cycles that switch between hosts such as *Trypanosoma cruzei*
89 and *Entamoeba histolytica* (16,17). Very little is known about the role of Q in bacterial pathogens that also
90 switch between mammalian and insect hosts such as the intracellular pathogen *Bartonella henselae*. This
91 bacterium uses fleas and possibly ticks as vectors during blood feeding. Feces of these insects can also
92 infect cats when they are scratched into a break in the skin. Once inside the cat, the bacteria enter the
93 bloodstream, primarily residing within endothelial cells, where they multiply (18). *B. henselae* exhibits a

94 high level of heterogeneity (19) and 16S rRNA sequence analyses led to the identification of two serotypes,
95 Houston-1 and Marseille (20,21). Metabolic reconstruction of the Q synthesis pathway of *B. henselae*
96 Houston 1 suggested it utilized a direct q salvage pathway like *C. trachomatis*. However, analysis of *B.*
97 *henselae* TGT and QTPR sequences did not match this prediction as these were more similar to the bTGT
98 and QPTR enzymes that recognize $preQ_1$. To resolve this discrepancy, we set out to characterize
99 experimentally the Q salvage enzymes in this facultative intracellular pathogen.

100

101 **Results**

102 **Metabolic reconstruction and sequence analyses of queuosine salvage genes give contradictory**
103 **results.**

104 We previously showed that QPTR proteins have different substrate specificities, shifting from $preQ_0$ and
105 $preQ_1$ in *E. coli* to q in *C. trachomatis* (14,15). To better understand the molecular determinants that drive
106 this change in specificity, we constructed a Sequence Similarity Network (SSN) of the QPTR family
107 (PF02592). We then colored the SSN based on the presence/absence of the Q synthesis genes in the
108 corresponding genome as an indirect way to predict the substrate specificity of a given QPTR protein. As
109 shown in Fig. 2, we were able to generate an SSN that separated the QPTR's predicted to salvage $preQ_0$
110 and $preQ_1$ (in yellow or red) from those predicted to salvage q (in blue) (Fig. 2). However, a few exceptions
111 stood out even at a stringent alignment score of 70. The QPTRs found in organisms that encode only *tgt*,
112 and hence predicted to salvage q, cluster with QPTR proteins predicted to salvage $preQ_0$/ $preQ_1$ because
113 their genomes encode QueA and QueG or QueH (circled in Fig. 2). These include QPTR proteins from
114 *Bartonella* species such as *B. henselae* Houston-1 (UniProt id A0A0H3M726_BARHE).

115 Following up on this discrepancy, we retrieved all Q synthesis proteins from the InterPro database
116 with their IPR protein family ID (see Materials and Methods) and counted the numbers of each protein
117 encoded in each genome at the level of different taxonomic ranks, including order, class, and family (Table
118 S1). Then, we extracted the TGT sequences from all orders, classes, families, and genera that encode only

119 *tgt* as described in the methods section, aligned them, and compared the predicted substrate-binding
120 residues (Table S2). As we previously reported (15), TGTs that salvage q typically contains GG[LS][AS]G
121 in the substrate-binding pocket (Fig. 3). Interestingly, TGTs in *Bartonella* and *Pelagibacter* contain a
122 GGLAVG site like the *E. coli* enzyme (Fig. 3) and are phylogenetically distant from other TGTs found in
123 genomes that only encode *tgt* (Fig. 3). We then examined the substrate-binding pocket in a modeled
124 structure of *B. henselae* TGT (Bh TGT, UniProt ID A0A0R4J8M4_BARHE) aligned with the structure of
125 the human TGT catalytic subunit QTRT1 in complex with q (PDB ID: 6H45) (22). The aspartate residues
126 and G216GLAVGE222 that are conserved in TGT proteins of the *Hyphomicrobiales* order are in proximity
127 to queuine (Fig. S1B and C). The predicted distance between V220 and the cis-diol groups of q is less than
128 1 Angstrom (Fig. S1C), suggesting that it may prevent the binding of q to *B. henselae* TGT as in the *Z.*
129 *mobilis* TGT (23). We previously showed that *C. trachomatis* TGT salvages q and that its substrate-binding
130 pocket can accommodate the larger substrate (15). Here, we propose that the TGT protein and the QPTR
131 transporter in *Bartonella* and *Pelagibacter* species salvage preQ$_1$, even though they lack, like *C.*
132 *trachomatis*, the enzymes that make Q-tRNAs from preQ$_1$-tRNAs.
133
134 ***B. henselae* TGT and QPTR proteins preferentially salvage preQ$_1$ but also q and Q with low affinity.**
135 The gene encoding the *B. henselae* Bh TGT protein complemented the Q- phenotype of a *queDF tgt* deletion
136 mutant of *E. coli* when expressed *in trans* and in the presence of exogenous preQ$_1$ even in low
137 concentrations (down to 10 nM). (Fig. 4). Similarly, Bh QPTR transported both preQ$_1$ and preQ$_0$ in an *E.*
138 *coli* strain auxotrophic for preQ$_1$ and preQ$_0$ (Fig. 4). These results confirmed our predictions based on the
139 SSN that the *Bartonella* TGT and QPTR proteins use preQ$_1$ as a substrate but do not match the metabolic
140 reconstruction that predicted q salvage in *B. henselae*. Hence, we tested if this organism's TGT and QPTR
141 could have evolved a broader substrate specificity and use q as a substrate.
142 To test whether the QPTR and TGT proteins of *B. henselae* can use q as a substrate, we used an *E.*
143 *coli* strain that expresses the QPTR and/or the TGT proteins of *C. trachomatis* that can only use q as a
144 substrate (Fig. 1) (15). Salvage of q was observed when expressing both Bh *tgt* and *yhhQ* genes at

145 concentrations of q over 500 nM (Fig. S3A). When overexpressing the *E. coli yhhQ* gene, no such salvage
146 of q was observed even at concentrations of 5 μM (Fig. S3A). However, if the *C. trachomatis* TGT and
147 QPTR proteins can salvage q when present at 100 nM, the Bh QPTR cannot (Fig. S2). These results showed
148 that the Bh QPTR protein has acquired the capacity to transport q while retaining the $preQ_1/preQ_0$
149 specificity, but it is still not as efficient as the *C. trachomatis* QPTR transporter that is specific for q.
150 We then tested whether the Bh QPTR could transport the Q ribonucleoside by taking advantage of
151 an *E. coli* strain expressing the *C. difficile* Q hydrolase (Cd *queK*) and q lyase (Cd *queL*) genes that allow
152 Q to be salvaged by *E. coli* (Fig. 1) (15). Expressing only Bh QPTR allowed the salvage of Q only at
153 extremely high concentrations (5 μM) (Fig. S3B). When the *C. difficile* Q transporter (Cd ECF_TAA',
154 QueT) is expressed in this strain, Q can be salvaged when present at concentrations of 100 nM [(15) and
155 (Fig. S3B].
156
157 **Traces of $preQ_1$ can be detected in endogenous *B. henselae* tRNAs**
158 The natural habitat of this intracellular pathogen (mammalian vasculature) should be richer in q than in
159 $preQ_1$. We, therefore, analyzed by LC-MS/MS the tRNA modification profile of bulk tRNA extracted from
160 *B. henselae* cells grown in HIBB medium. The experiments were performed three times independently with
161 conflicting results. The first two experiments were done to test the tRNA extraction protocols with an
162 intracellular bacterium, using only one sample each time. Small amounts of $preQ_1$ and minute amounts of
163 Q were detected the first time (but neither was present the second time (data not shown). Because cells were
164 grown in the presence of sheep blood and serum, we had little control over the sources of Q or $preQ_1$; we,
165 therefore, repeated the experiment a third time with 5 independent samples, adding 100 nM $preQ_1$ in three
166 of the samples. As shown in Fig. 5, Fig. S4 and Table S3, small amounts of $preQ_1$ and Q were detected in
167 all samples (around 1000 times less than in a typical *E. coli* sample). The exogenous addition of 100 nM
168 $preQ_1$ did not make any difference. It is not possible to determine if the observed Q was derived from *B.*
169 *henselae* tRNAs or from contaminating mammalian tRNAs, as eukaryotic-specific tRNA modifications

170 such as $m^2{}_2G$, are detected in similar quantities (Table S3) and great variations in Q levels were observed
171 between samples. Nevertheless, the presence of $preQ_1$ cannot be explained by any contamination, and these
172 results identify $preQ_1$ as the final product for the first time in a naturally occurring organism since it had
173 only been detected previously in *queA* mutants of *E. coli* (24). The low amounts detected suggest that the
174 tRNAs are not fully modified, as the $preQ_1$ levels are 11%-40% of $cmnm^5s^2U$ levels and 1.1%-2.8% of k^2C
175 levels two well conserved bacterial modifications (25)(Fig. S5 and Table S3).
176

177 **Early loss of Q pathway genes in the *Bartonellaceae* family within the *Hyphomicrobiales* order**

178 *B. henselae* belongs to the Alphaproteobacteria class (25). This is a diverse Gram-negative taxon comprised
179 of several phototrophic genera, several genera metabolizing C1-compounds (e.g., *Methylobacterium* spp.),
180 symbionts of plants (e.g., *Rhizobium* spp.), endosymbionts of arthropods (*Wolbachia*) and intracellular
181 pathogens (e.g., *Rickettsia*) (26). To better understand the evolution of the Q synthesis and salvage pathway
182 in Alphaproteobacteria, we performed a phylogenetic distribution analysis of the corresponding genes in
183 2,127 different species with complete genome sequences from the class in the BV-BRC database as
184 described in the methods section (Fig. S6). The tree suggests that there were three events involving the loss
185 of $preQ_1$ synthesis genes: one occurred after the split between *Brucella* and *Bartonella* species (Fig. 6 and
186 Fig. S6 node 1), one occurred after the split of *Pelagibacteraceae* (Fig. S6 and Fig S7 node 2), and one
187 occurred after the split of *Anaplasmataceae* (Fig. S6 and Fig S7 node 3). This analysis revealed that most
188 Alphaproteobacteria are prototrophic for Q, as 1,414 (64%) of the species analyzed encode the complete
189 pathway. In addition, if the loss of the $preQ_1$ synthesis genes occurred sporadically in different branches,
190 all the organisms analyzed, with the exception of *Bartonella,* harbored *tgt*, *queA*, and *queG* genes and hence
191 were not predicted to salvage q. Focusing more specifically on the *Bartonella* genus using a similar analysis
192 revealed a very different pattern (Fig. 6).

193 Among the 65 organisms in the *Bartonella* genus with available complete genomes, as of October
194 2023, only *Bartonella* sp. HY038, branching at the root of the genus, encoded the canonical *de novo* Q
195 synthesis pathway. Most, like *B. henselae*, have lost all the genes but *tgt*. In addition, a more in-depth

196 analysis revealed fragmented *tgt* genes of several *B. quintana* strains (boxed in Fig. 6), suggesting these
197 organisms have totally lost the capacity to make Q-modified tRNAs. This evolutionary scenario seems to
198 be a recurring theme in intracellular bacteria as seen in the *Rickettsiales*. While nearly all rickettsiae
199 branching closer to the root retain the full pathway except for *queD* (collapsed in Fig. S7), other rickettsiae
200 such as *Anaplasma, Ehrlichia,* and *Wolbachia*, have lost nearly the full pathway. However, cases of
201 fragmented *tgt* genes are rare and only observed in a *Wolbachia* endosymbiont of *Cimex lectularius* (box
202 in Fig. S6).

203 In summary, the phylogenic distribution analysis suggests that the direct ancestor of *Bartonella*
204 species must have harbored the full Q pathway but that it was lost very early in the evolution of this clade.
205 Most bacteria in this clade are predicted to transport and insert $preQ_1$ but without further conversion to Q.
206 In addition, some species like *B. quintana* have lost the pathway completely (Fig. 6).

207

208 **Discussion**

209 Q is an ancient modification predicted to be present in the ancestors of bacteria (27). It is still present in
210 most extant bacteria even if minimalist genetic codes can exist without this complex modification (28).
211 Independent analyses of the genomes of bacteria in the human microbiome have shown that 90 to 95% of
212 these organisms maintain the capacity to synthesize or salvage Q with around half encoding the full
213 synthesis pathway (15,29). Many of the bacteria that have lost Q are organisms that have undergone a
214 genome reduction process, where their genetic material has been streamlined over evolutionary time such
215 as the parasitic *Mycoplasma* spp. or insect endosymbionts such as *Riesia pediculicola* (30,31).

216 Obligate intracellular human pathogens tend to have reduced genomes compared to their free-living
217 ancestors as their metabolisms have adapted to a nutritionally rich niche (32). Regarding Q, the scenarios
218 that one can envision in the transition to a strict intracellular lifestyle with access to the queuine precursor
219 from the mammalian host are: 1) keeping the ancestral pathway; 2) losing the modification; or 3) switching
220 to a queuine salvage route. We performed the metabolic reconstruction of Q metabolism in genera of strict
221 intracellular human pathogens such as Chlamydia spp., members of the order Rickettsiales (*Anaplasma*

222 spp., and *Rickettsia* spp.) and *Coxiella burnetii* (33,34). Indeed, examples of these three possible paths were
223 observed (Fig. 7): Rickettsia (Fig. 7A) and Coxiella (Table S5 line 267) have kept the full Q synthesis
224 pathway; *Anaplasma* spp. (Fig. 7A), *Borrelia* (Fig. 7B), *Ehrlichia* spp. (Table S5 line 52), and Chlamydia
225 (Table S5 line 212), kept only *tgt*. Most species in the class of Mycobacteriales have totally lost the pathway
226 genes except *tgt* (Fig. 7C).

227 The situation seen in *B. henselae* is not commonly observed in other intracellular bacteria and no
228 other organisms in the Hyphomicrobiales order seem to follow the same pattern (Fig. 7D). Indeed, the
229 presence of TGT and QPTR homologs and the absence of QueA and QueG or QueH (Fig. 6) would suggest
230 that these organisms salvage q like *C. trachomatis*, but the corresponding enzymes have retained their
231 substrate specificity towards $preQ_1$ (Fig. 3 and 4). $PreQ_1$ is not a molecule found in mammalian cells (Brian
232 Green, personal communication), and the fact that we were able to detect a small proportion of tRNAs
233 carrying that modification when extracted from *B. henselae* cells grown in sheep blood agar (HIBB)
234 suggests this pathway is functional even if the source of $preQ_1$ remains a mystery and could be due to
235 contamination with a $preQ_1$ synthesizing organism, an unknown source of $preQ_1$ in the culture medium, or
236 on the activity of a yet-to-be-discovered q hydrolase (intracellular or possibly extracellular as q transport
237 is not efficient as discussed below) (Fig. 1D). The low amount of $preQ_1$ modification (Table S3) suggests
238 it does not play an important role in decoding accuracy under these conditions. The fact that *tgt* gene decay
239 is observed in several organisms in this clade such as *B. quintana* reinforces this idea. A primary difference
240 between *B. quintana* and *B. henselae* is their reservoir ecology. *B. quintana* uses only humans as a reservoir,
241 whereas *B. henselae* is more promiscuous and frequently isolated from both cats and humans (35).

242 Another intriguing finding of this study is that the QPTR and TGT enzymes of *B. henselae* can use
243 q as a substrate when present at high concentrations (>500 nM), whereas the E. coli orthologs cannot. It is
244 difficult to establish if such concentrations could be physiological, and we could not show with certainty
245 that *B. henselae* tRNA extracted from HIBB-grown cells harbored Q. One can propose several evolutionary
246 explanations for this broadening of substrate specificity of the *B. henselae* salvage proteins. In one, the
247 enzyme and transporter specificities would become more relaxed in *B. henselae* as they are no longer under

248 selective pressure to maintain efficient $preQ_1$ selection, and we are observing an intermediate stage along
249 the loss of the whole pathway. An argument against that hypothesis is that if $preQ_1$ synthesis genes and
250 *queA*, *queG* and *queH* genes seem to have been lost very early in the clade, *tgt* is often the last maintained
251 and we did not find any examples where *tgt* was lost with the other genes maintained, suggesting a fitness
252 advantage of maintaining the *tgt* gene. The other possibility is that we are observing a transition of a $preQ_1$
253 salvage to a q salvage that is working poorly in human cells but could be efficient in an environment with
254 more q/Q. Could the insect vector provide such an environment? Answering these questions will require
255 further studies, including additional quantitative data on q/$preqQ_1$ levels in different environments and
256 tRNA modification profiles along the pathogen's life cycle. In summary, the study sheds light on the diverse
257 and adaptable nature of queuosine metabolism in various bacteria, particularly in intracellular pathogens.
258 The unique characteristics of Q salvage observed in *B. henselae* raise intriguing questions about its role in
259 different host/vector environments. Further investigations are warranted to unravel the complexities of Q
260 salvage and its implications to Bartonella's virulence.
261

262 **Materials and methods**

263 **Comparative genomics and bioinformatics**

264 The BLAST tools (36) resources at the National Center for Biotechnology Information (NCBI) and BV-
265 BRC (37) were routinely used. Multiple sequence alignments were built using MUSCLE v5. 1 (38) and
266 visualized and edited with Jalview2 (39). Protein sequences were retrieved from the NCBI using the
267 following accession numbers: Ct yhhQ, NP_219643.1; Ct tgt, NP_219697.1; Cd ECF-A, YP_001086568.1;
268 Cd ECF-A, YP_001086569.1; Cd ECF-T, YP_001086570.1; Cd Queuosine hydrolase, YP_001088185.1;
269 Cd ECF-S, YP_001088186.1; Cd Queuine lyase, YP_001088187.1; Ec yhhQ, WP 001100469.1; Ec tgt; Bh
270 yhhQ, WP_011181356.; Bh tgt, WP_011180873.1. Protein IDs used for this study are listed in Table S6.
271 Complete genomes of Alphaproteobacteria with good quality were retrieved from BV-BRC (37).

272 For metabolic reconstruction analyses in each taxonomic rank, all protein members were retrieved
273 from the InterPro database (40) using the following IPR family ID: FolE1, IPR001474; FolE2, IPR003801;

274 QueD, IPR007115; QueE, IPR024924; QueC, IPR018317; QueF, IPR00029500; TGT, IPR004803; QueA,
275 IPR003699; QueG, IPR004453; QueH, IPR003828. A universal single copy small ribosomal protein uS2,
276 (IPR001865) was used to estimate the number of organisms in each rank. The number of proteins per
277 taxonomic rank was computed and the criteria used for filtering the groups ranks encoding just TGT were
278 the following: 1) the number of TGT proteins was no less than 10 so we were not polluted with small
279 taxonomic sample size; 2) the number of each of the QueDECFAGH proteins was no more than a fifth of
280 the number of TGT proteins. To analyze the conserved residues in the substrate-binding pockets, the
281 sequences of TGT proteins from select taxonomic groups were retrieved from UniProt and aligned using
282 MUSCLE v5.1 (38). The Conserved residues were visualized using weblogo3 (41).
283 The structure of TGT proteins (*Bartonella henselae* str. Houston-1 TGT, A0A0R4J8M4;
284 *Anaplasma phagocytophilum* TGT, S6G6J1; *Nakamurella multipartita* TGT, C8X7A7) were modeled
285 using SWISS-MODEL (39) using Alpha Fold structure (*Bartonella fuyuanensis* TGT (ID
286 A0A840DZ06_9HYPH), *Anaplasma phagocytophilum* str ApMUC09 TGT (ID A0A0F3NAG3_ANAPH),
287 and *Nakamurella multipartita* TGT (ID C8X7A7_NAKMY) as templates respectively (42). The cartoon
288 representation of protein structure was produced by PyMol (version 2.5) (43) and colored by domain (red,
289 N-terminus; light blue, C-terminus).
290
291 **Sequence Similarity Networks (SSNs)**
292 The Enzyme Function Initiative (EFI) suite of web tools was used to generate the SSN (44). Visualization
293 of SSNs was carried out using Cytoscape 3.10.1ape (45). 7,625 PF02592 family sequences were retrieved
294 from UniProt using the family option with fraction of 3 and submitted to EFI. The initial SSN was generated
295 with an alignment score cutoff set such that each connection (edge) represents a sequence identity of above
296 approximately 40%. The obtained SSN was first colored according to the configurations for salvaging
297 $preQ_1$, $preQ_0$, queuine, and Queuosine *de novo* synthesis. Then more stringent SSNs were created by
298 increasing the alignment score cutoff in small increments (usually by 5). This process was repeated until
299 most clusters were homogeneous in their colors. The UniProt IDs were associated with the genome ID

300 including GenBank/EMBL, RefSeq nucleotide, BV-BRC genome ID, Ensembl genome ID, using
301 homemade scripts (scripts available upon request). The UniProt IDs of PF02592 family sequences in the
302 SSN are listed in Table S7 as well as corresponding presence of Q pathway genes. The connection between
303 UniProt IDs and genome information was performed by querying UniProt ID mapping file using homemade
304 scripts (scripts available upon request).
305
306 **Phylogenetic investigations and Q gene presence/absence distribution pattern analysis**
307 For phylogenetic analysis of species, the 20 ribosomal protein data (L2, L3, L4, L5, L6, L9, L10, L14, L16,
308 L18, L22, L24, S2, S3, S4, S5, S8, S10, S17, and S19) were retrieved from BV-BRC and aligned
309 independently using MUSCLE v5.1 (38). Alignments were trimmed using BMGE v1.12 using default
310 settings (46) and then concatenated. To build the phylogenetic tree of TGT proteins, the sequences of TGT
311 proteins from each taxonomic rank were retrieved (ID are listed in Table S6) and subject to alignment with
312 MUSCLE (39) and trimming with BMGE (46). The maximum likelihood tree was built by FastTree (47)
313 using the LG-cat model with a hundred bootstraps. Trees were visualized using iTOL (48). To view the
314 gene clustering near *tgt* in different bacterial genomes, GizmoGene (http://www.gizmogene.com) was used
315 to extract gene regions and subjected to visualization using Gene Graphics (49). The genomic regions are
316 listed in Table S4.
317
318 **Strains, media, and growth conditions**
319 Strains and plasmids used in this study are listed in Table S9. LB medium (tryptone 10 grams/liter, yeast
320 extract 5 grams/liter, sodium chloride 5 grams/liter) was routinely used for *E. coli* strain growth at 37°C.
321 The medium was solidified using 15 g/L of agar. As needed, kanamycin (50 g/mL), ampicillin (100 g/mL),
322 and chloramphenicol (25 g/mL) were added. In the presence of exogenous Q precursors as previously
323 described (50), cells were cultured in M9-defined medium containing 1% glycerol (Thermo Fisher
324 Scientific, Waltham, MA, USA) for the purpose of eliminating background Q-tRNA. After cells reached
325 an optical density at 600 nm (OD_{600nm}) of 0.1-0.2, 0.2% arabinose was added to induce the expression of

326 genes under the pBAD promoter. After cells reached an OD_{600nm} of 0.2, DMSO, $preQ_0$, $preQ_1$, q, or Q were
327 added. The transport reaction was stopped at time points of 30 or 60 min after supplementing with DMSO
328 or different Q precursors by placing samples on melting ice and then centrifuging, followed by tRNA
329 extraction. Q was purchased from Epitoire (Singapore), q from Santa Cruz Biotechnology, $preQ_1$ and $preQ_0$
330 from Sigma-Aldrich.

331 *B. henselae* Houston I was obtained from the American Type Culture Collection (ATCC 49882)
332 and cultivated as previously described (51) on HIBB agar plates [Bacto heart infusion agar (Becton,
333 Dickinson, Sparks, MD)] supplemented with 4% defibrinated sheep blood and 2% sheep serum (Quad Five,
334 Ryegate, MT) by volume] for 4 days at 37°C, 5% CO_2 and 100% relative humidity. When required, $preQ_1$
335 was added to a final concentration of 100 nM. Following harvest into ice-cold heart infusion broth, tRNA
336 was collected from the bacterial cells.

337

338 **Construction of *E. coli* strains and plasmids**

339 *B. henselae yhhQ* gene (Bh *yhhQ*) was chemically synthesized (without optimization) in pTWIST-Kan
340 vector. XbaI and HindIII restrictions sites were added at the 5′ and 3′ ends, respectively (Twist Bioscience
341 HQ) (**Table S10**). Bh *yhhQ* DNA sequence was amplified using two primers pairs (F_Bh
342 yhhQ_XbaI_PBAD33 and R_Bh yhhQ_HindIII_PBAD33) by PCR with the addition of restrictions
343 sites XbaI and HindIII at their 5′ and 3′ ends, respectively. Bh *yhhQ* was cloned into the XbaI and HindIII
344 sites of pBAD33. *B. henselae tgt* (Bh *tgt*) was amplified by PCR from *B. henselae* genomic DNA using
345 the KpnI-RBS-TGTBh-F_PBAD24 and TGTBh-SbfI-R _PBAD24 primers and cloned into the KpnI and
346 SbfI sites of pBAD24. The UniProt IDs for Bh *yhhQ* and Bh *tgt* are A0A0H3M726_BARHE and
347 A0A0R4J8M4_BARHE, respectively. *E. coli* transformations were performed using the $CaCl_2$ chemical
348 transformation procedure (52). Transformants were selected on LB agar supplemented with ampicillin or
349 chloramphenicol (100 µg/mL). The clones were validated through sequencing and PCR analyses using
350 primers designed specifically for Bh *yhhQ* and Bh *tgt* genes. All primers used in this study are listed in
351 Table S10.

352

353 **tRNA extraction and migration**

354 Cells were harvested by centrifugation at 16,000 x g for 2 minutes at 4°C. Immediately after pelleting, the
355 cells were resuspended in 1 mL of Trizol (Thermo Fisher Scientific, Waltham, MA, USA). According to
356 the manufacturer's instructions, small RNA was extracted with the PureLink^{Tm} miRNA Isolation kit
357 (Thermo Fisher Scientific, Waltham, MA, USA). 50 µL of RNase-free water were used to elute the purified
358 RNAs. Quantification of prepared tRNA was performed using a Nanodrop 1000 spectrophotometer. We
359 loaded 150 ng of tRNAs per well on a denaturing 8 M urea, 8% polyacrylamide gel containing 0.5% 3-
360 (Acrylamido) phenylboronic acid (Sigma-Aldrich) after resuspending in a 2X RNA Loading Dye (NEB).
361 Migration was performed in a mixture of 1X TAE at 4°C. With a wet transfer apparatus in 1X TAE at 150
362 mA at 4°C for 90 minutes, tRNAs were transferred onto a Biodyne B precut nylon membrane (Thermo
363 Scientific). The membrane was UV irradiated in a UV crosslinker (Fisher FB-UVXL-1000) at a preset UV
364 energy dosage of 120 mJ/cm2. The North2South Chemiluminescent Hybridization and Detection Kit
365 (Thermo) was used to detect tRNA^{Asp}. As the DIG Easy Hyb (Roche) drastically reduces the background
366 noise, it was used as the initial membrane-blocking buffer instead of the North2South kit's membrane-
367 blocking buffer. Hybridization was done at 60°C, using the specific biotinylated primer for tRNA Asp GUC
368 (14) (5' biotin-CCCTCGGTGACAGGCAGG 3' for *E. coli* added to a final concentration of 50 ng/mL.
369 The blot was visualized by the iBright™ Imaging Systems.

370

371 **tRNA profiling by mass spectrometry**

372 tRNA for each sample (1.8 µg) was hydrolyzed in a 30 µL digestion cocktail containing 2.49 U benzonase,
373 3 U CIAP (calf intestinal alkaline phosphatase), 0.07 U PDE I (phosphodiesterase I), 0.1 mM deferoxamine,
374 0.1 mM BHT (butylated hydroxytoluene), 3 ng coformycin, 25 nM 15N-dA (internal standard $[^{15}N]_5$-
375 deoxyadenosine), 2.5 mM $MgCl_2$ and 5 mM Tris-HCL buffer pH 8.0. The digestion mixture was incubated
376 at 37 °C for 6 h. After digestion, all samples were analyzed by chromatography-coupled triple-quadrupole
377 mass spectrometry (LC-MS/MS). For each sample, 600 ng of hydrolysate was injected for two technical

replicates. Using synthetic standards, HPLC retention times of RNA modifications were confirmed on a Waters Acuity BEH C18 column (50 × 2.1 mm inner diameter, 1.7 µm particle size) coupled to an Agilent 1290 HPLC system and an Agilent 6495 triple-quad mass spectrometer. The Agilent sample vial insert was used. The HPLC system was operated at 25 °C and a flow rate of 0.3 mL/min in a gradient Table S11 with Buffer A (0.02% formic acid in double distilled water) and Buffer B (0.02% formic acid in 70% acetonitrile). The HPLC column was coupled to the mass spectrometer with an electrospray ionization source in positive mode with the following parameters: Dry gas temperature, 200 °C; gas flow, 11 L/min; nebulizer, 20 psi; sheath gas temperature, 300 °C; sheath gas flow, 12 L/min; capillary voltage, 3000 V; nozzle voltage, 0 V. Multiple reaction monitoring (MRM) mode was used for detection of product ions derived from the precursor ions for all the RNA modifications with instrument parameters including the collision energy (CE) optimized for maximal sensitivity for the modification. Based on synthetic standards (Biosynth) with optimized collision energies, the following transitions and retention times (except k^2C, which we do not have standard) were monitored: $cmnm^5s^2U$, m/z 348 → 141, 2.36 min; k^2C, m/z 372.1 → 240.1; $m^{2,2}G$, m/z 312 → 180, 9.70 min; $preQ_1$, m/z 312 → 163, 2.15 min; Q, m/z 410 → 163, 5.53 min. Signal intensities for each ribonucleoside were normalized by dividing by the sum of the UV signal intensities of the four canonical ribonucleosides recorded with an in-line UV spectrophotometer at 260 nm.

Acknowledgments

This work was funded by the National Institutes of Health (project numbers GM070641, ES026856, and ES024615) and the National Research Foundation of Singapore through the Singapore-MIT Alliance for Research and Technology Antimicrobial Resistance Interdisciplinary Research Group. We are also thankful to Dr Brian Greene for communicating unpublished results.

402 **References**

403 1. El Yacoubi B, Bailly M, de Crécy-Lagard V. Biosynthesis and function of posttranscriptional
404 modifications of transfer RNAs. Annu Rev Genet. 2012 Dec 15;46(1):69–95.
405 2. Antoine L, Bahena-Ceron R, Bunwaree HD, Gobry M, Loegler V, Romby P, et al. RNA
406 modifications in pathogenic bacteria: Impact on host adaptation and virulence. Vol. 12, Genes.
407 MDPI AG; 2021. p. 1125.
408 3. Fleming BA, Blango MG, Rousek AA, Kincannon WM, Tran A, Lewis AJ, et al. A tRNA modifying
409 enzyme as a tunable regulatory nexus for bacterial stress responses and virulence. Nucleic Acids
410 Res. 2022 Jul 22;50(13):7570–90.
411 4. Hutinet G, Swarjo MA, de Crécy-Lagard V. Deazaguanine derivatives, examples of crosstalk
412 between RNA and DNA modification pathways. Vol. 14, RNA Biology. Taylor and Francis Inc.;
413 2017. p. 1175–84.
414 5. Fergus C, Barnes D, Alqasem MA, Kelly VP. The queuine micronutrient: Charting a course from
415 microbe to man. Vol. 7, Nutrients. MDPI AG; 2015. p. 2897–929.
416 6. Zallot R, Brochier-Armanet C, Gaston KW, Forouhar F, Limbach PA, Hunt JF, et al. Plant, animal,
417 and fungal micronutrient queuosine is salvaged by members of the DUF2419 protein family. ACS
418 Chem Biol. 2014 Aug 15;9(8):1812–25.
419 7. Chevance FFV, Le Guyon S, Hughes KT. The effects of codon context on in vivo translation speed.
420 PLoS Genet. 2014;10(6):e1004392.
421 8. Whittle CA, Kulkarni A, Chung N, Extavour CG. Adaptation of codon and amino acid use for
422 translational functions in highly expressed cricket genes. BMC Genomics. 2021 Dec 1;22(1):234.
423 9. Pollo-Oliveira L, Davis NK, Hossain I, Ho P, Yuan Y, Salguero García P, et al. The absence of the
424 queuosine tRNA modification leads to pleiotropic phenotypes revealing perturbations of metal and
425 oxidative stress homeostasis in *Escherichia coli* K12. Metallomics. 2022 Sep 24;14(9):mfac065.

426 10. Durand JM, Dagberg B, Uhlin BE, Björk GR. Transfer RNA modification, temperature and DNA
427 superhelicity have a common target in the regulatory network of the virulence of *Shigella flexneri*:
428 the expression of the *virF* gene. Mol Microbiol. 2000;35(4):924–35.
429 11. Díaz-Rullo J, González-Pastor JE. tRNA queuosine modification is involved in biofilm formation
430 and virulence in bacteria. Nucleic Acids Res. 2023 Aug 28;51(18):9821–37.
431 12. Fruchard L, Babosan A, Carvalho A, Lang M, Li B, Duchateau M, et al. Queuosine modification of
432 tRNA-Tyrosine elicits translational reprogramming and enhances growth of *Vibrio cholerae* with
433 aminoglycosides. bioRxiv 2022 Jan 1;2022.09.26.509455. Available from:
434 http://biorxiv.org/content/early/2022/09/26/2022.09.26.509455.abstract
435 13. Zallot R, Ross R, Chen WH, Bruner SD, Limbach PA, de Crécy-Lagard V. Identification of a novel
436 epoxyqueuosine reductase family by comparative genomics. ACS Chem Biol. 2017 Feb
437 8;12(3):844–51.
438 14. Zallot R, Yuan Y, De Crécy-Lagard V. The *Escherichia coli* COG1738 member YhhQ is involved
439 in 7-cyanodeazaguanine ($preQ_0$) transport. Biomolecules. 2017 Mar 1;7(1):12.
440 15. Yuan Y, Zallot R, Grove TL, Payan DJ, Martin-Verstraete I, Šepić S, et al. Discovery of novel
441 bacterial queuine salvage enzymes and pathways in human pathogens. Proc Natl Acad Sci U S A.
442 2019 Sep 17;116(38):19126–35.
443 16. Guillén N. Pathogenicity and virulence of *Entamoeba histolytica*, the agent of amoebiasis. Vol. 14,
444 Virulence. 2023. p. 2158656.
445 17. Dixit S, Kessler AC, Henderson J, Pan X, Zhao R, D'Almeida GS, et al. Dynamic queuosine changes
446 in tRNA couple nutrient levels to codon choice in *Trypanosoma brucei*. Nucleic Acids Res. 2021
447 Dec 16;49(22):12986–99.
448 18. Jin X, Gou Y, Xin Y, Li J, Sun J, Li T, et al. Advancements in understanding the molecular and
449 immune mechanisms of Bartonella pathogenicity. Front Microbiol. 2023 Jul 27;14:1196700.

450 19. Hansmann Y, DeMartino S, Piémont Y, Meyer N, Mariet P, Heller R, et al. Diagnosis of cat scratch
451 disease with detection of *Bartonella henselae* by PCR: A study of patients with lymph node
452 enlargement. J Clin Microbiol. 2005 Aug;43(8):3800–6.
453 20. La Scola B, Liang Z, Zeaiter Z, Houpikian P, Grimont PAD, Raoult D. Genotypic characteristics of
454 two serotypes of *Bartonella henselae*. J Clin Microbiol. 2002;40(6):2002–8.
455 21. Zeaiter Z, Fournier PE, Raoult D. Genomic variation of *Bartonella henselae* strains detected in
456 lymph nodes of patients with cat scratch disease. J Clin Microbiol. 2002;40(3):1023–30.
457 22. Johannsson S, Neumann P, Ficner R. Crystal structure of the human tRNA guanine transglycosylase
458 catalytic subunit QTRT1. Biomolecules. 2018 Sep 1;8(3):81.
459 23. Stengl B, Reuter K, Klebe G. Mechanism and substrate specificity of tRNA-Guanine
460 transglycosylases (TGTs): tRNA-modifying enzymes from the three different kingdoms of life share
461 a common catalytic mechanism. Chem Bio Chem 2005;6(11):1926–39.
462 24. Slany RK, Bosl M, Kersten H. Transfer and isomerization of the ribose moiety of AdoMet during
463 the biosynthesis of queuosine tRNAs, a new unique reaction catalyzed by the QueA protein from
464 *Escherichia coli*. Biochimie [Internet]. 1994;76(5):389–93. Available from:
465 http://research.bmn.com/medline/search/results?uid=MDLN.95151848
466 25. Boccaletto P, MacHnicka MA, Purta E, Pitkowski P, Baginski B, Wirecki TK, et al. MODOMICS:
467 A database of RNA modification pathways. 2017 update. Nucleic Acids Res. 2018;46(D1):D303–
468 7.
469 26. Ferla MP, Thrash JC, Giovannoni SJ, Patrick WM. New rRNA gene-based phylogenies of the
470 Alphaproteobacteria provide perspective on major groups, mitochondrial ancestry and phylogenetic
471 instability. PLoS One. 2013 Dec 11;8(12):e83383.
472 27. Cermakian N, Cedergren R. Modified nucleosides always were: an evolutionary model. In: Grosjean
473 H, Benne R, editors. Modification and Editing of RNA. Washington, D. C.: ASM Press; 1998. p.
474 535–41.

475 28. Garzón MJ, Reyes-Prieto M, Gil R. The minimal translation machinery: what we can learn from
476 naturally and experimentally reduced genomes. Front Microbiol. 2022;13:858983.
477 29. Yan F, Xiang S, Shi L, Zhu X. Synthesis of queuine by colonic gut microbiome via cross-feeding.
478 Food Frontiers1. 2023 Sep 15;1–14.
479 30. Grosjean H, Breton M, Sirand-Pugnet P, Tardy F, Thiaucourt F, Citti C, et al. Predicting the minimal
480 translation apparatus: lessons from the reductive evolution of Mollicutes. PLoS Genet. 2014;10(5).
481 31. de Crécy-Lagard V, Marck C, Grosjean H. Decoding in Candidatus *Riesia pediculicola*, close to a
482 minimal tRNA modification set? Trends Cell Mol Biol 2012];7:11–34.
483 32. Murray GGR, Charlesworth J, Miller EL, Casey MJ, Lloyd CT, Gottschalk M, et al. Genome
484 reduction Is associated with bacterial pathogenicity across different scales of temporal and
485 ecological divergence. Mol Biol Evol. 2021;38(4):1570–9.
486 33. McClure EE, Chávez ASO, Shaw DK, Carlyon JA, Ganta RR, Noh SM, et al. Engineering of
487 obligate intracellular bacteria: Progress, challenges and paradigms. Vol. 15, Nature Reviews
488 Microbiology. 2017. p. 544–58.
489 34. Loterio RK, Zamboni DS, Newton HJ. Keeping the host alive - Lessons from obligate intracellular
490 bacterial pathogens. Vol. 79, Pathogens and Disease. 2021. p. ftab052.
491 35. Alsmark CM, Frank AC, Karlberg EO, Legault BA, Ardell DH, Canbäck B, et al. The louse-borne
492 human pathogen *Bartonella quintana* is a genomic derivative of the zoonotic agent *Bartonella*
493 *henselae*. Proc Natl Acad Sci U S A. 2004;101(26):9716–21.
494 36. Altschul SF, Madden TL, Schaffer AA, Zhang J, Zhang Z, Miller W, et al. Gapped BLAST and PSI-
495 BLAST: a new generation of protein database search programs. Nucleic Acids Res.
496 1997;25(17):3389–402.
497 37. Olson RD, Assaf R, Brettin T, Conrad N, Cucinell C, Davis JJ, et al. Introducing the Bacterial and
498 Viral Bioinformatics Resource Center (BV-BRC): a resource combining PATRIC, IRD and ViPR.
499 Nucleic Acids Res. 2023 Jan 6;51(D1):D678–89.

500 38. Edgar RC. Muscle5: High-accuracy alignment ensembles enable unbiased assessments of sequence
501 homology and phylogeny. Nat Commun. 2022 Nov 15;13(1):6968.
502 39. Waterhouse AM, Procter JB, Martin DMA, Clamp M, Barton GJ. Jalview Version 2-A multiple
503 sequence alignment editor and analysis workbench. Bioinformatics. 2009;25(9):1189–91.
504 40. Paysan-Lafosse T, Blum M, Chuguransky S, Grego T, Pinto BL, Salazar GA, et al. InterPro in 2022.
505 Nucleic Acids Res. 2023 Jan 6;51(D1):D418–27.
506 41. Crooks GE, Hon G, Chandonia JM, Brenner SE. WebLogo: A Sequence Logo Generator. Genome
507 Res. 2004;14(6):1188–90.
508 42. Varadi M, Anyango S, Deshpande M, Nair S, Natassia C, Yordanova G, et al. AlphaFold Protein
509 Structure Database: Massively expanding the structural coverage of protein-sequence space with
510 high-accuracy models. Nucleic Acids Res. 2022 Jan 7;50(D1):D439–44.
511 43. Zhu K, Day T, Warshaviak D, Murrett C, Friesner R, Pearlman D. Antibody structure determination
512 using a combination of homology modeling, energy-based refinement, and loop prediction. Proteins:
513 Structure, Function and Bioinformatics. 2014;82(8):1646–55.
514 44. Gerlt JA, Bouvier JT, Davidson DB, Imker HJ, Sadkhin B, Slater DR, et al. Enzyme function
515 initiative-enzyme similarity tool (EFI-EST): A web tool for generating protein sequence similarity
516 networks. Vol. 1854, Biochimica et Biophysica Acta - Proteins and Proteomics. Elsevier B.V.; 2015.
517 p. 1019–37.
518 45. Shannon P, Markiel A, Ozier O, Baliga NS, Wang JT, Ramage D, et al. Cytoscape: A software
519 Environment for integrated models of biomolecular interaction networks. Genome Res. 2003
520 Nov;13(11):2498–504.
521 46. Criscuolo A, Gribaldo S. BMGE (Block Mapping and Gathering with Entropy): a new software for
522 selection of phylogenetic informative regions from multiple sequence alignments. BMC Evol Biol.
523 2010/07/16. 2010;10:210.
524 47. Price MN, Dehal PS, Arkin AP. FastTree 2 – approximately maximum-likelihood trees for large
525 alignments. PLoS One. 2010 Mar 10;5(3):e9490.

526 48. Letunic I, Bork P. Interactive tree of life (iTOL) v5: An online tool for phylogenetic tree display
527 and annotation. Nucleic Acids Res. 2021;49(W1):W293–6.
528 49. Harrison KJ, de Crécy-Lagard V, Zallot R. Gene Graphics: A genomic neighborhood data
529 visualization web application. Bioinformatics. 2018;34(8):1406–8.
530 50. Kelley LA, Mezulis S, Yates CM, Wass MN, Sternberg MJE. The Phyre2 web portal for protein
531 modeling, prediction and analysis. Nat Protoc. 2015 Jun 30;10(6):845–58.
532 51. Battisti JM, Minnick MF. Laboratory maintenance of *Bartonella quintana*. Curr Protoc Microbiol.
533 2008 Aug;10(1):3C.1.1-3C.1.13.
534 52. Green R, Rogers EJ. Transformation of chemically competent *E. coli*. In: Methods in Enzymology.
535 Academic Press Inc.; 2013. p. 329–36.
536
537
538
539
540
541
542
543
544
545
546
547
548
549
550
551

552 **Figure legends**

553

554 **Fig 1. Known or predicted Q synthesis pathways.**

555 (A) $preQ_0$/$preQ_1$ synthesis and salvage pathways in *E. coli*; (B) q salvage pathway in *C. trachomatis*; (C)
556 $preQ_1$, q and Q salvage pathways in *C. difficile*. The ECF transporters include 4 subunits: S, the substrate-
557 specific transmembrane component (QueT); T, the energy-coupling module; A and A', a pair of ABC
558 ATPase. (D) Possible q and Q salvage pathways in *B. henselae* Houston 1.

559

560 **Figure 2. Protein sequence similarity network (SSN) of 7,625 QPTR (PF02592 family) proteins.**

561 Each node in the network represents a QPTR protein. An edge (represented as a line) is drawn between two
562 nodes with a BLAST *E*-value cutoff of better than 10^{-70} (alignment score of 70). The nodes are colored
563 based on the presence/absence of the other Q synthesis genes in the corresponding genome. Cases with
564 inconclusive Q pathway gene distribution are colored in light gray. QPTR proteins without genome
565 information are colored in dark gray. QPTR homologs from *E. coli* and *C. trachomatis* are indicated by
566 yellow and blue arrows, respectively. The solitary TGTs from genomes harboring only *tgt* that cluster with
567 TGTs in complete Q pathways are circled in blue.

568

569 **Figure 3. Comparison of the phylogenetic tree of taxonomic ranks of bacteria that harbor *tgt* only**
570 **and the maximum likelihood tree of their TGT proteins.**

571 The maximum likelihood tree of marker proteins of taxonomic ranks of bacteria that harbor *tgt* only without
572 other Q proteins (left). The maximum likelihood tree of TGT proteins from organisms of each
573 corresponding rank (right). Human and tRNA-guanine (15) transglycosylase from *P. horikoshii* were used
574 as the outgroup for each tree, respectively. TGT of *E. coli* was used for comparison. Bootstraps above 0.5
575 are shown under the branch. A multiple sequence alignment of consensus residues in the TGT proteins in
576 the moiety of 7-substitue of deazapurine is shown (middle). The residues are highlighted by the percent

577 identity. The dashed lines connect each organism and their TGT sequence. The branch of TGTs from
578 *Bartonella, Pelagibacter, E. coli*, and humans is highlighted in red.
579
580 **Figure 4. Bh TGT and Bh YhhQ salvage preQ$_1$ in *E. coli*.**
581 Detection of Q-tRNAAsp GUC by the APB assay. Q-modified tRNAs that migrate slower are indicated by
582 an arrow. tRNAs were extracted from WT and mutant strains expressing different Q salvage genes. The
583 strains used are denoted in the first line. The genes and corresponding vectors are indicated in the second
584 line. Plasmid and strain information are given in Table S9. Cells were grown in minimal media in the
585 presence of exogenous preQ$_0$ and preQ$_1$. DMSO was used as control when no preQ$_0$ and preQ$_1$ was
586 supplemented.
587
588 **Figure 5. Normalized peak area values of preQ$_1$ and Q in *B. henselae*.**
589 600 ng of hydrolysate was injected for LC-MS/MS. For each condition, two technical replicates were
590 performed for each sample. The signals were confirmed by both qualifier and quantifier transitions. preQ$_1$
591 and Q were detected in all samples. There is significant difference for preQ$_1$ between BH-WT_17 and BH-
592 WT+preQ1_21 sample, but not in other samples. Q showed significant difference between BH-WT and
593 BH-WT+preQ$_1$, however, the trend is uncertain since the "biological replicates" showed variable results.
594 Data represent the means ±SD for 2 technical replicates. Statistical analysis was done by one-way analysis
595 of variance (ANOVA) with prism 9, $p < 0.05$ and $p < 0.01$ are denoted as * and ** respectively. All
596 modifications were validated with standards.
597
598 **Figure 6. Phylogenetic Analysis of Queuosine Biosynthesis Genes in Bartonellaceae.** The clade of
599 *Bartonella spp.* (*Bartonellaceae*; Alphaproteobacteria; left). The branches of *Pseudochrobactrum,*
600 *Brucella*, and *Ochrobactrum* were collapsed. The highlighted node 1 corresponds to the node in the tree in
601 Figure S6. The presence of Q biosynthesis proteins is indicated by the circles with TGTs highlighted in red.
602 The comparative view of the corresponding truncated and full-length *tgt* gene variants in different

603 *Bartonella* species in the tree (right). Red, *tgt*; yellow, *queA*; blue, genes encoding a transporter-like protein;
604 black, hypothetical genes; gray, other genes. The fragmented *tgt* genes in *B. quintana* strains are boxed.
605 Gene IDs are provided in supplementary Table S4.
606
607 **Figure 7. The prevalence of Q pathway proteins in selected taxonomic ranks in Uniprot database.**
608 (A) A cladogram of the order Hyphomicrobiales. (B) A cladogram of the order Mycobacteriales. (C) A
609 cladogram of the class Spirochaetia. (D) A cladogram of the order Rickettsiales. Each pie chart represents
610 the percentage of organisms in each taxonomic rank that contains the corresponding Q pathway protein.
611 The size of each triangle correlates with the number of genomes in each taxonomic unit. The sequences of
612 TGTs' substrate binding sites from ranks that encoded only *tgt* were analyzed and presented in Table. S2.
613 Only taxonomic ranks that contain more than 15 TGTs are shown.
614
615
616
617

Figure 1

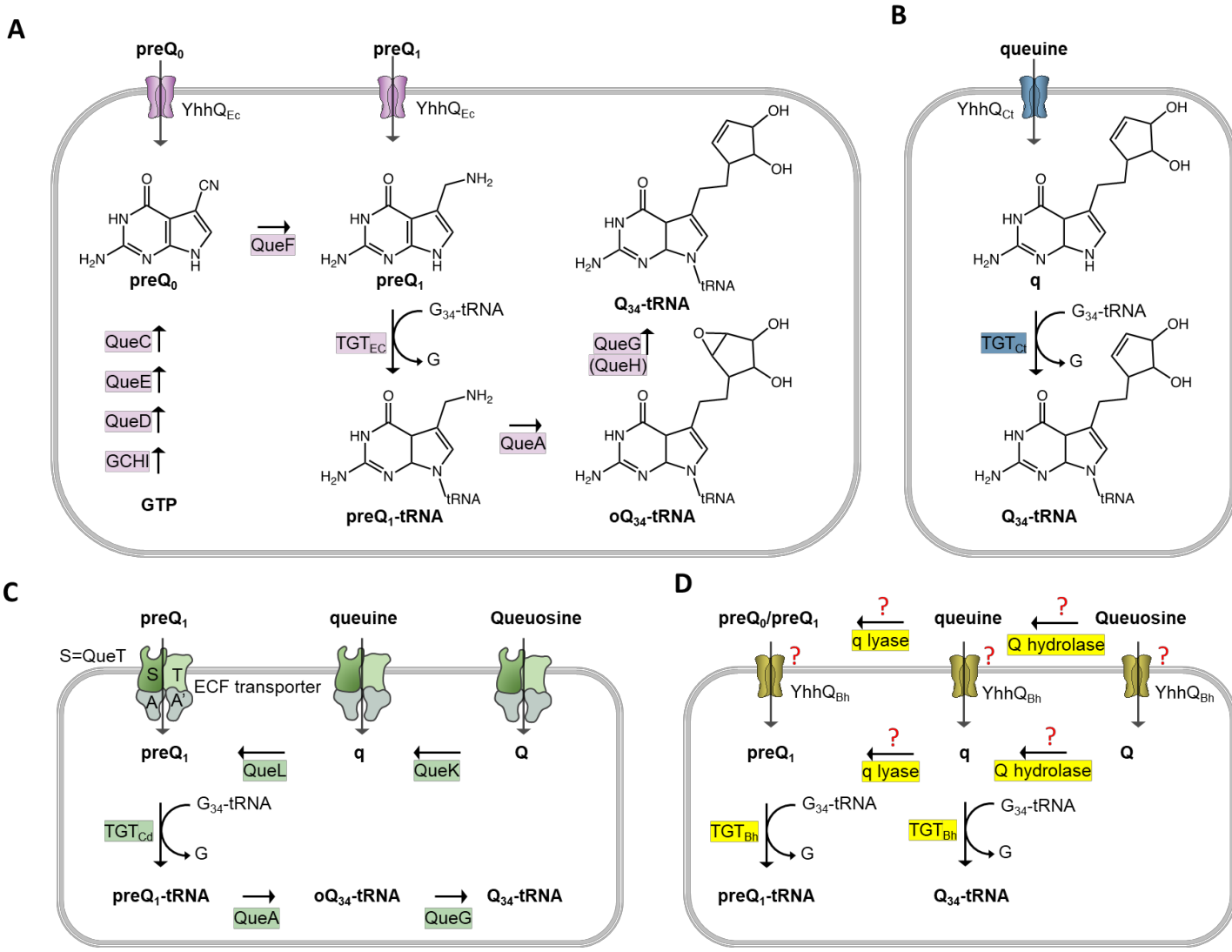

A
preQ0
preQ1
YhhQEc
YhhQEc
preQ0
QueF
preQ1
Q34-tRNA
QueC
QueE
QueD
GCHI
GTP
TGTEC
G34-tRNA
G
QueG
(QueH)
QueA
preQ1-tRNA
oQ34-tRNA
B
queuine
YhhQCt
q
TGTCt
G34-tRNA
G
Q34-tRNA
C
preQ1
queuine
Queuosine
S=QueT
ECF transporter
preQ1
QueL
q
QueK
Q
TGTCd
G34-tRNA
G
preQ1-tRNA
QueA
oQ34-tRNA
QueG
Q34-tRNA
D
preQ0/preQ1
q lyase
queuine
Q hydrolase
Queuosine
YhhQBh
YhhQBh
YhhQBh
preQ1
q lyase
q
Q hydrolase
Q
TGTBh
G34-tRNA
G
TGTBh
G34-tRNA
G
preQ1-tRNA
Q34-tRNA

Figure 2

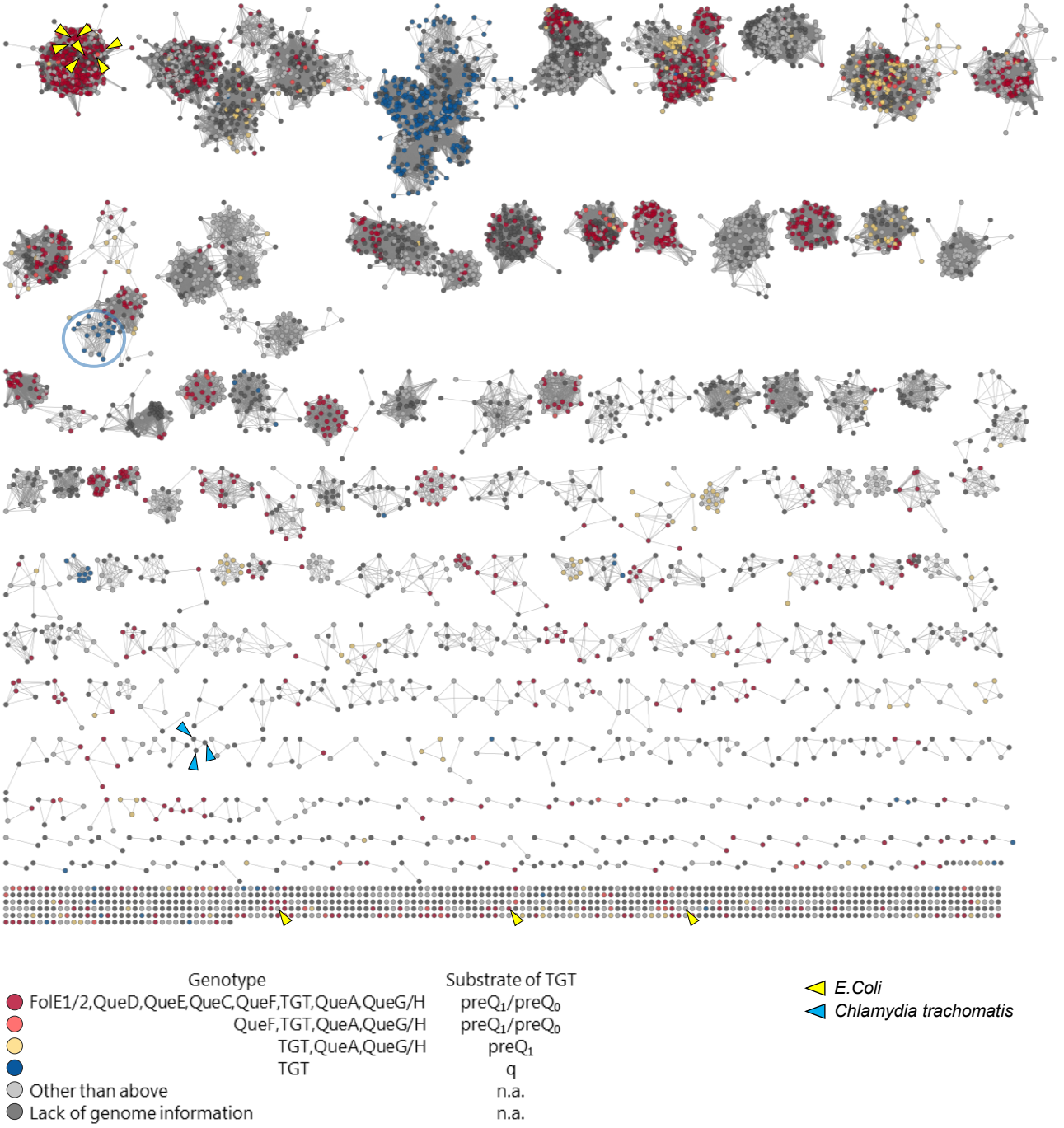
Genotype
Substrate of TGT
FolE1/2,QueD,QueE,QueC,QueF,TGT,QueA,QueG/H
preQ1/preQ0
QueF,TGT,QueA,QueG/H
preQ1/preQ0
TGT,QueA,QueG/H
preQ1
TGT
q
Other than above
n.a.
Lack of genome information
n.a.
E.Coli
Chlamydia trachomatis

Figure 3

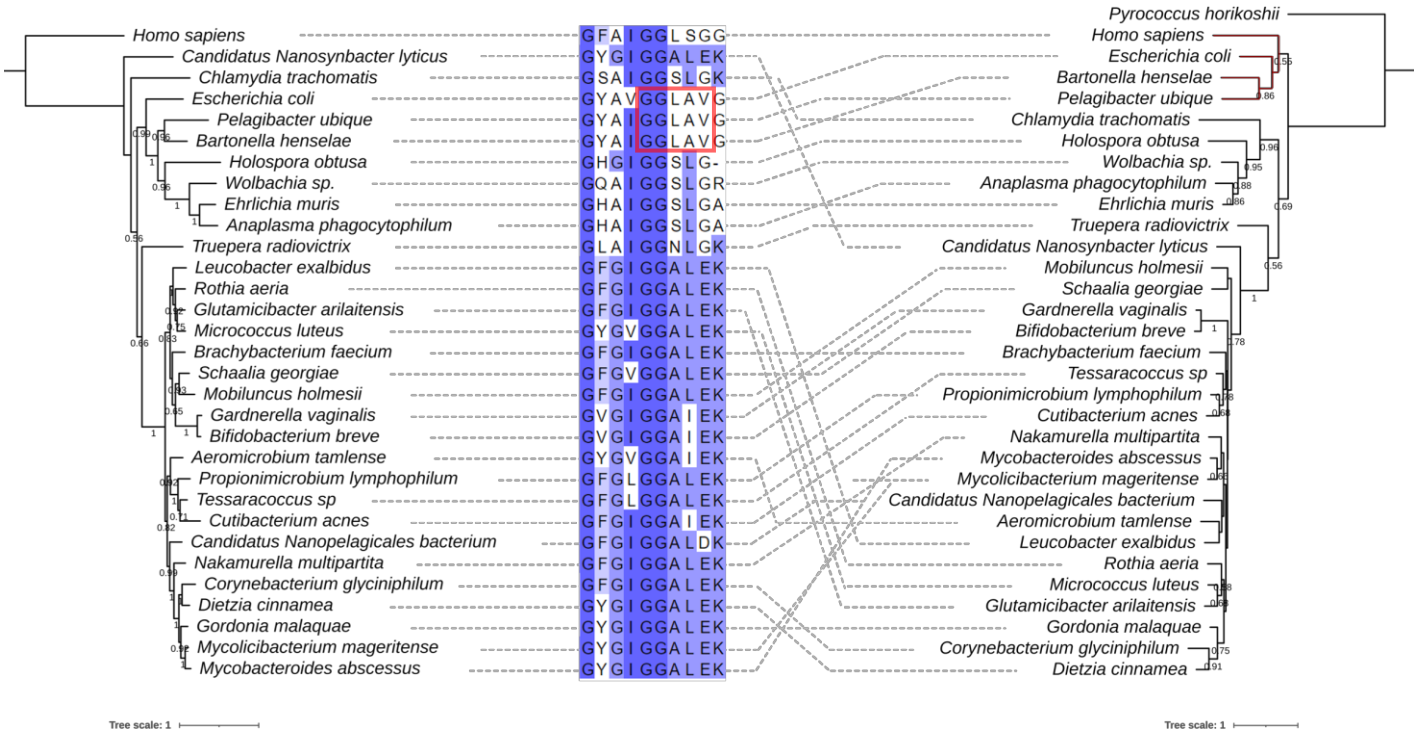
Homo sapiens
Candidatus Nanosynbacter lyticus
Chlamydia trachomatis
Escherichia coli
Pelagibacter ubique
Bartonella henselae
Holospora obtusa
Wolbachia sp.
Ehrlichia muris
Anaplasma phagocytophilum
Truepera radiovictrix
Leucobacter exalbidus
Rothia aeria
Glutamicibacter arilaitensis
Micrococcus luteus
Brachybacterium faecium
Schaalia georgiae
Mobiluncus holmesii
Gardnerella vaginalis
Bifidobacterium breve
Aeromicrobium tamlense
Propionimicrobium lymphophilum
Tessaracoccus sp
Cutibacterium acnes
Candidatus Nanopelagicales bacterium
Nakamurella multipartita
Corynebacterium glyciniphilum
Dietzia cinnamea
Gordonia malaquae
Mycolicibacterium mageritense
Mycobacteroides abscessus
Pyrococcus horikoshii
Tree scale: 1
Tree scale: 1

Figure 4

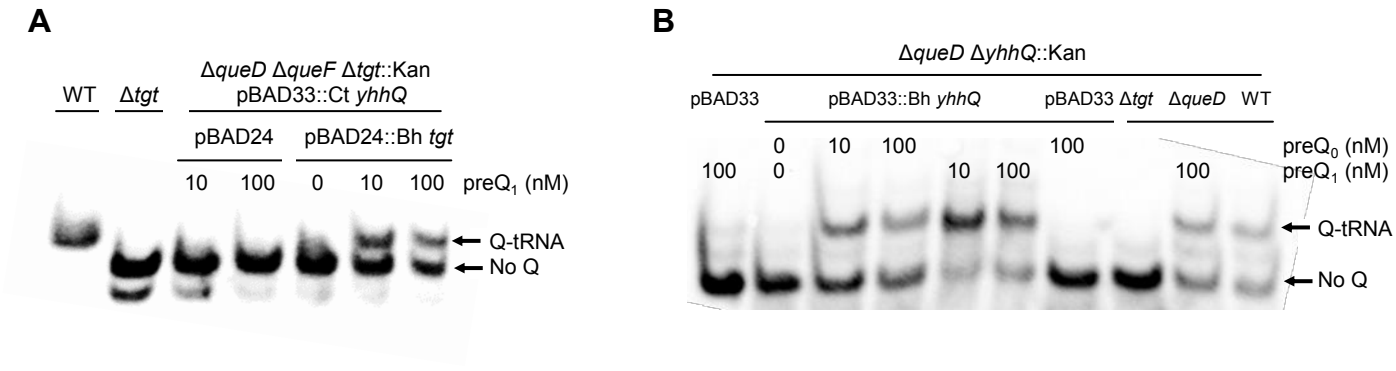
A
WT
Δtgt
ΔqueD ΔqueF Δtgt::Kan
pBAD33::Ct yhhQ
pBAD24
pBAD24::Bh tgt
10
100
0
10
100
preQ1 (nM)
Q-tRNA
No Q
B
ΔqueD ΔyhhQ::Kan
pBAD33
pBAD33::Bh yhhQ
pBAD33
Δtgt
ΔqueD
WT
0
10
100
100
preQ0 (nM)
100
0
10
100
100
preQ1 (nM)
Q-tRNA
No Q

Figure 5

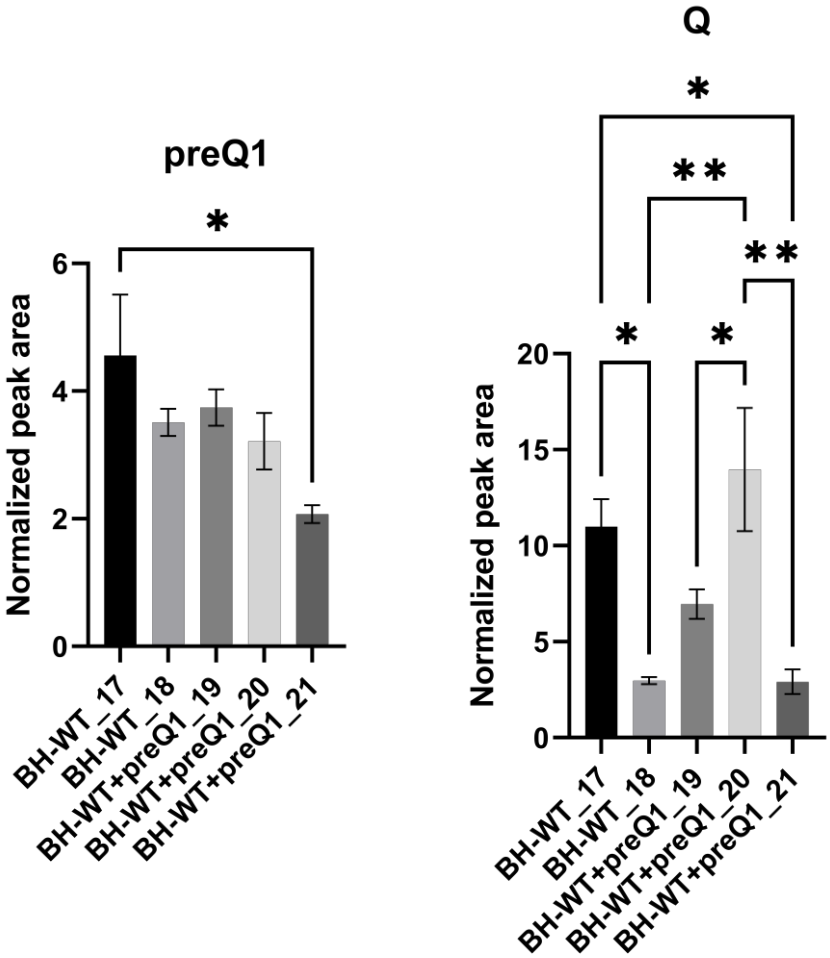
preQ1
Normalized peak area
0
2
4
6
*
BH-WT_17
BH-WT_18
BH-WT+preQ1_19
BH-WT+preQ1_20
BH-WT+preQ1_21
Q
Normalized peak area
0
5
10
15
20
*
**
**
*
*
BH-WT_17
BH-WT_18
BH-WT+preQ1_19
BH-WT+preQ1_20
BH-WT+preQ1_21

Figure 6

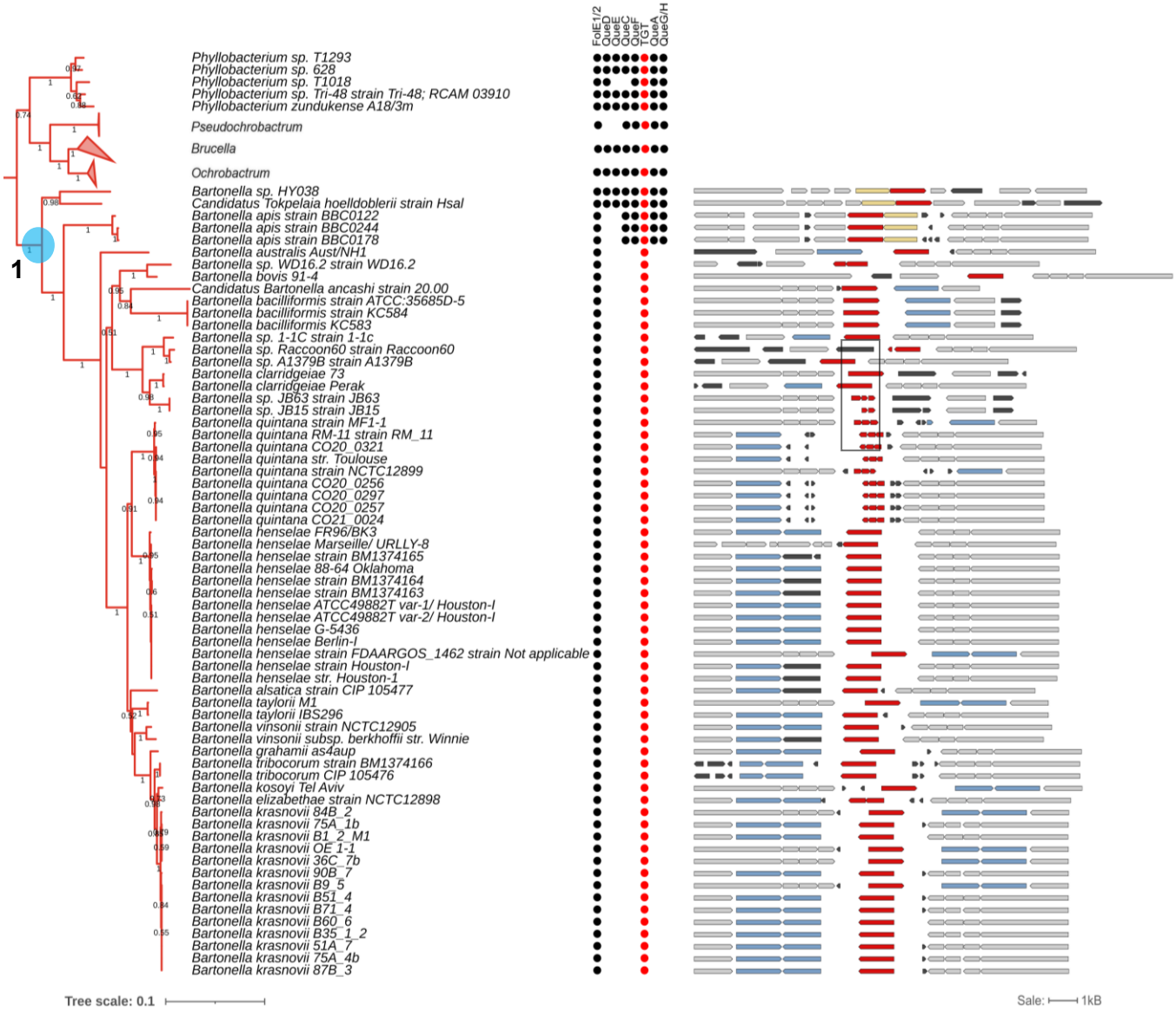
FolE1/2
QueD
QueE
QueC
QueF
FGT
QueA
QueG/H
Phyllobacterium sp. T1293
Phyllobacterium sp. 628
Phyllobacterium sp. T1018
Phyllobacterium sp. Tri-48 strain Tri-48; RCAM 03910
Phyllobacterium zundukense A18/3m
Pseudochrobactrum
Brucella
Ochrobactrum
Bartonella sp. HY038
Candidatus Tokpelaia hoelldoblerii strain Hsal
Bartonella apis strain BBC0122
Bartonella apis strain BBC0244
Bartonella apis strain BBC0178
Bartonella australis Aust/NH1
Bartonella sp. WD16.2 strain WD16.2
Bartonella bovis 91-4
Candidatus Bartonella ancashi strain 20.00
Bartonella bacilliformis strain ATCC:35685D-5
Bartonella bacilliformis strain KC584
Bartonella bacilliformis KC583
Bartonella sp. 1-1C strain 1-1c
Bartonella sp. Raccoon60 strain Raccoon60
Bartonella sp. A1379B strain A1379B
Bartonella clarridgeiae 73
Bartonella clarridgeiae Perak
Bartonella sp. JB63 strain JB63
Bartonella sp. JB15 strain JB15
Bartonella quintana strain MF1-1
Bartonella quintana RM-11 strain RM_11
Bartonella quintana CO20_0321
Bartonella quintana str. Toulouse
Bartonella quintana strain NCTC12899
Bartonella quintana CO20_0256
Bartonella quintana CO20_0297
Bartonella quintana CO20_0257
Bartonella quintana CO21_0024
Bartonella henselae FR96/BK3
Bartonella henselae Marseille/ URLLY-8
Bartonella henselae strain BM1374165
Bartonella henselae 88-64 Oklahoma
Bartonella henselae strain BM1374164
Bartonella henselae strain BM1374163
Bartonella henselae ATCC49882T var-1/ Houston-I
Bartonella henselae ATCC49882T var-2/ Houston-I
Bartonella henselae G-5436
Bartonella henselae Berlin-I
Bartonella henselae strain FDAARGOS_1462 strain Not applicable
Bartonella henselae strain Houston-I
Bartonella henselae str. Houston-1
Bartonella alsatica strain CIP 105477
Bartonella taylorii M1
Bartonella taylorii IBS296
Bartonella vinsonii strain NCTC12905
Bartonella vinsonii subsp. berkhoffii str. Winnie
Bartonella grahamii as4aup
Bartonella tribocorum strain BM1374166
Bartonella tribocorum CIP 105476
Bartonella kosoyi Tel Aviv
Bartonella elizabethae strain NCTC12898
Bartonella krasnovii 84B_2
Bartonella krasnovii 75A_1b
Bartonella krasnovii B1_2_M1
Bartonella krasnovii OE 1-1
Bartonella krasnovii 36C_7b
Bartonella krasnovii 90B_7
Bartonella krasnovii B9_5
Bartonella krasnovii B51_4
Bartonella krasnovii B71_4
Bartonella krasnovii B60_6
Bartonella krasnovii B35_1_2
Bartonella krasnovii 51A_7
Bartonella krasnovii 75A_4b
Bartonella krasnovii 87B_3
1
Tree scale: 0.1
Sale: 1kB

Figure 7

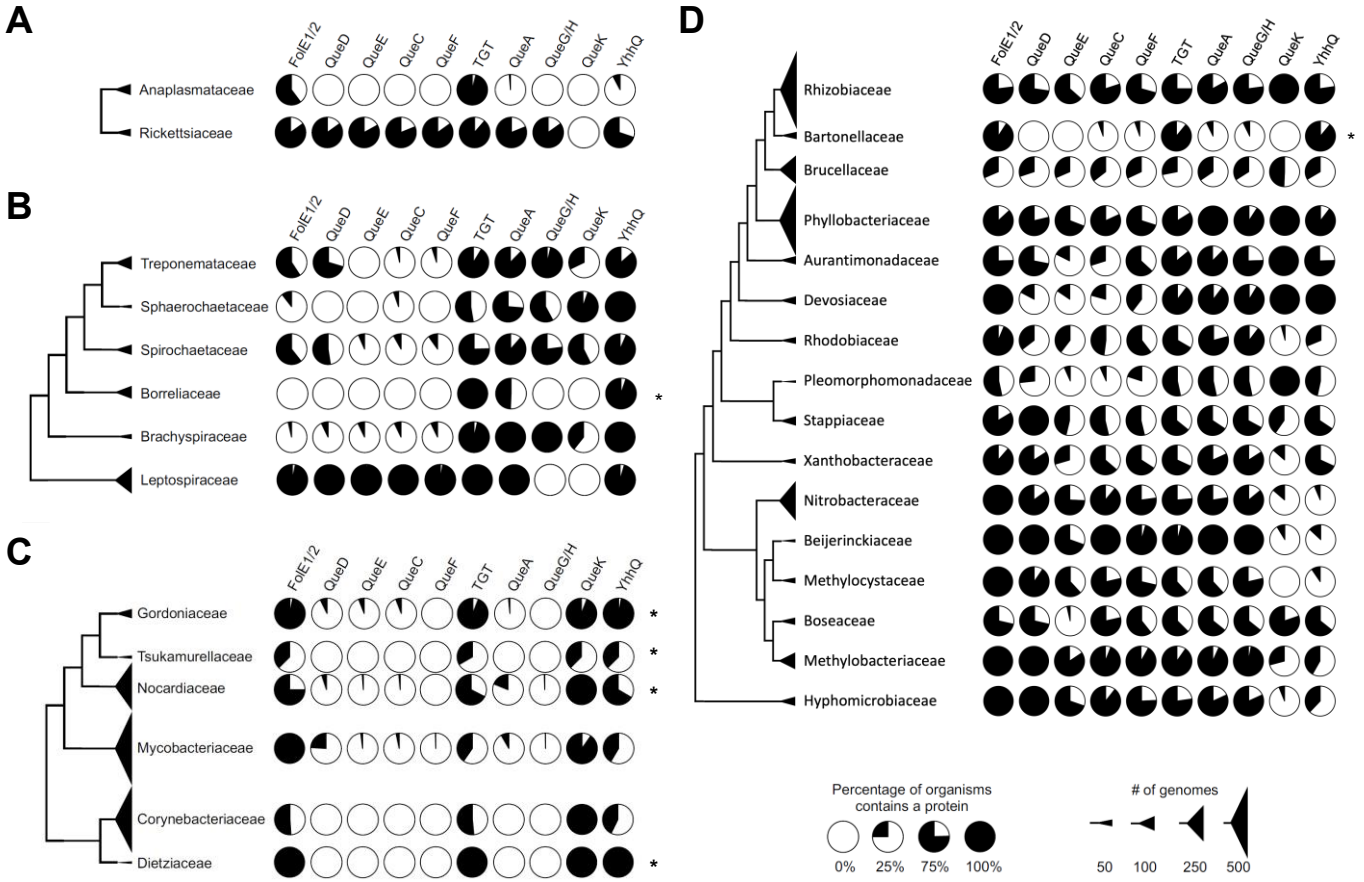
A
FolE1/2
QueD
QueE
QueC
QueF
TGT
QueA
QueG/H
QueK
YhhQ
Anaplasmataceae
Rickettsiaceae
B
Treponemataceae
Sphaerochaetaceae
Spirochaetaceae
Borreliaceae
Brachyspiraceae
Leptospiraceae
C
Gordoniaceae
Tsukamurellaceae
Nocardiaceae
Mycobacteriaceae
Corynebacteriaceae
Dietziaceae
D
Rhizobiaceae
Bartonellaceae
Brucellaceae
Phyllobacteriaceae
Aurantimonadaceae
Devosiaceae
Rhodobiaceae
Pleomorphomonadaceae
Stappiaceae
Xanthobacteraceae
Nitrobacteraceae
Beijerinckiaceae
Methylocystaceae
Boseaceae
Methylobacteriaceae
Hyphomicrobiaceae
Percentage of organisms contains a protein
0%
25%
75%
100%
# of genomes
50
100
250
500